

DOE/ER/40537--87

# Entrance Channel Dependent Light-Charged Particle Emission of the $^{156}\text{Er}$ Compound Nucleus

J. F. Liang, J. D. Bierman, M. P. Kelly, A. A. Sonzogni, R. Vandenbosch and J.P.S. van Schagen  
*Nuclear Physics Laboratory, Box 354290 University of Washington Seattle, WA 98195*  
 (June 18, 1996)

RECEIVED

SEP 09 1996

OSTI

Light-charged particle decay from the  $^{156}\text{Er}$  compound nucleus, populated by  $^{12}\text{C}+^{144}\text{Sm}$  and  $^{60}\text{Ni}+^{96}\text{Zr}$  at the same excitation energy, were measured in coincidence with the evaporation residues. The high energy slope of charged particle spectra for the  $^{60}\text{Ni}$ -induced reaction is steeper than for the  $^{12}\text{C}$ -induced reaction. Model calculations including particle evaporation during compound nucleus formation result in good agreement with the data. This suggests that the difference in the charged particle spectra between the two entrance channels is due to a longer formation time in the  $^{60}\text{Ni}$ -induced reaction.

PACS number(s): 24.60.Dr, 25.70.Gh, 25.70.-z

The time scales for large scale rearrangement of nuclear matter is one of the important problems in nuclear physics. It is influenced by whether nuclear dissipation is primarily one-body or two-body. These issues can be probed in nuclear fission and fusion reactions [1]. Several experiments have been performed at excitation energies near 53–56 MeV to look for possible entrance channel effects in fusion reactions. When a compound nucleus is populated from entrance channels with significantly different formation times, one may be able to observe different behaviors in the decay of the compound nucleus. Mixed results were obtained. For instance, the spectrum of the high energy  $\gamma$ -rays from the decay of the giant dipole resonance built on excited states in  $^{164}\text{Yb}$  formed by  $^{64}\text{Ni}+^{100}\text{Mo}$  did not agree with statistical model calculations. Nevertheless no disagreement was observed in the same compound nucleus formed in the  $^{16}\text{O}+^{148}\text{Sm}$  reaction [2]. Another well studied case was the  $^{156}\text{Er}$  compound nucleus which was populated by two different entrance channels,  $^{12}\text{C}+^{144}\text{Sm}$  and  $^{64}\text{Ni}+^{92}\text{Zr}$ . The neutron multiplicities measured from the mass nearly symmetric entrance channel failed to meet the expectation from a statistical model, whereas for the  $^{12}\text{C}+^{144}\text{Sm}$  reaction the experimental data and model calculations are in good agreement [3]. However, the results of light-charged particle and  $\gamma$ -ray measurements were inconclusive [4].

It is assumed that a compound nucleus has no memory of its formation. In a statistical model, for a given excitation energy and angular momentum, the compound nucleus decay should be independent of the entrance channel [5]. Dynamical effects were introduced to explain the entrance channel dependence of the  $^{164}\text{Yb}$  data. It is

known that nuclear dissipation will prolong the fusion process in particular for the mass symmetric entrance channels [6]. If the compound nucleus formation time is longer than the lifetime of the dinuclear system, particle and  $\gamma$ -ray emission may take place before the system reaches equilibrium thus reducing the excitation energy of the compound nucleus. In Ref. [2], the  $\gamma$ -ray spectrum was reproduced by calculations taking into account particle evaporation and  $\gamma$ -ray emission during the formation stage.

In this letter, the study of light-charged particles emitted from the  $^{156}\text{Er}$  compound nucleus populated by two entrance channels is presented. The aim of the present experiment was to clarify the situation by going to higher excitation energies where the nuclear evaporation times, which serves as a clock, are an order of magnitude faster. In order to make comparisons between the two reactions, it is important to match the excitation energy and angular momentum. The angular momentum can be matched by populating the compound nucleus with a spin distribution well above the critical angular momentum ( $l_c^{ER}$ ) for evaporation residues (ERs). Partial waves with  $l$  greater than  $l_c^{ER}$  lead to fission and the latter quantity can be used as a cutoff in the spin distributions. In laboratory experiments, this can be achieved by measuring coincidences between the decay particles and ERs from a compound nucleus.

The experiments were carried out in the Nuclear Physics Laboratory at the University of Washington. The compound nucleus  $^{156}\text{Er}$  was populated by  $^{12}\text{C}+^{144}\text{Sm}$  and  $^{60}\text{Ni}+^{96}\text{Zr}$  at an average excitation energy of 113 MeV. The fission barriers at the maximum angular momentum of the reaction fall below the neutron binding energy. This gives a similar spin distribution for fusion leading to ERs for both systems. At such a high excitation energy, charged particle decay competes more effectively with neutron and  $\gamma$ -ray emission. Beams of  $^{12}\text{C}$  and  $^{60}\text{Ni}$  were produced by the tandem-linac accelerator and were incident on isotopically enriched  $^{144}\text{Sm}$  (200  $\mu\text{g}/\text{cm}^2$  on a 15  $\mu\text{g}/\text{cm}^2$  carbon foil) and  $^{96}\text{Zr}$  (1  $\text{mg}/\text{cm}^2$ , self-supporting) targets, respectively. Angular distributions of light-charged particles were measured by three CsI scintillators, coupled to PIN diode detectors, in coincidence with ERs. Light-charged particles were identified by pulse shape discrimination techniques. The CsI-PIN diode detectors were calibrated by elastic scattering of protons and  $\alpha$  particles. The linearity in energy

DISTRIBUTION OF THIS DOCUMENT IS UNLIMITED

ph

MASTER

response of the CsI crystal over the region of interest is excellent. ERs were separated from the beam by a pair of electrostatic deflectors and collected by a large area ( $6 \times 7 \text{ cm}^2$ ) silicon strip detector placed downstream. The identification of ERs was obtained by their time-of-flight and energy using the linac RF-clock as a reference.

The energy spectra of light-charged particles were transformed to the center of mass frame of the compound nucleus. For the same reaction, the spectral shape is nearly identical for all the angles ( $60^\circ$  to  $160^\circ$ ). Figure 1 shows the particle spectra for protons and  $\alpha$  particles in the center of mass frame. The dynamic range of the data extends over four decades. Only statistical uncertainties are presented in the figure. As can be seen, the light-charged particles emitted from the  $^{60}\text{Ni}$ -induced reaction are softer than those from the  $^{12}\text{C}$ -induced reaction. This suggests that for the  $^{60}\text{Ni}$ -induced reaction the particles were emitted from a colder source.

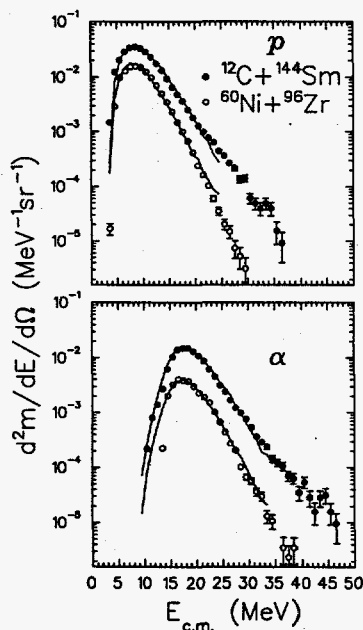


FIG. 1. Light-charged particle energy spectra for  $^{12}\text{C}+^{144}\text{Sm}$  and  $^{60}\text{Ni}+^{96}\text{Zr}$  at  $\theta_{lab} = 130^\circ$  and  $\theta_{lab} = 110^\circ$ , respectively. The proton spectra are shown in the upper panel and the  $\alpha$  particle spectra are in the lower panel. The results of statistical model calculations are shown by the solid curves.

The experiments were repeated several times by varying the geometries of the deflectors and detectors to investigate if there were biases in obtaining the coincidence data. In particular, one of the charged particle detectors was placed at  $90^\circ$  in the laboratory frame and on the same side as the residue detector with respect to the beam to simulate the worst configuration with respect to introducing problems of bias. Furthermore, the voltage of the electrostatic deflectors was varied to allow detecting different portions of the ER angular distributions. The spectral shape for the  $^{60}\text{Ni}$ -induced reaction is still

softer than that of the  $^{12}\text{C}$ -induced reaction.

Since the projectile energy for the  $^{12}\text{C}+^{144}\text{Sm}$  reaction is greater than 10 MeV per nucleon, it is necessary to consider the pre-equilibrium emission which is characterized by particle spectra with a very shallow slope and energies extending to several times the projectile energy per nucleon. Possible evidence for such a contribution can be seen in the proton spectrum of Fig. 1. A Fermi jet model [7] was used to estimate the contribution of pre-equilibrium emission. This estimate is rather uncertain at the very low bombarding energies employed in the present study as the model was developed for and is applicable at several tens of MeV per nucleon. The diffuseness of the Fermi momentum distribution was adjusted in the calculation to reproduce the highest energy part of the  $^{12}\text{C}+^{144}\text{Sm}$  data, as shown by the dash-dotted curves in Fig. 2. This calculation overestimates the contribution for  $^{60}\text{Ni}+^{96}\text{Zr}$  and should only be considered as an upper limit. When this component was subtracted from the particle spectra, the differences in the high energy slopes of the particle spectra for the two different entrance channels still persist.

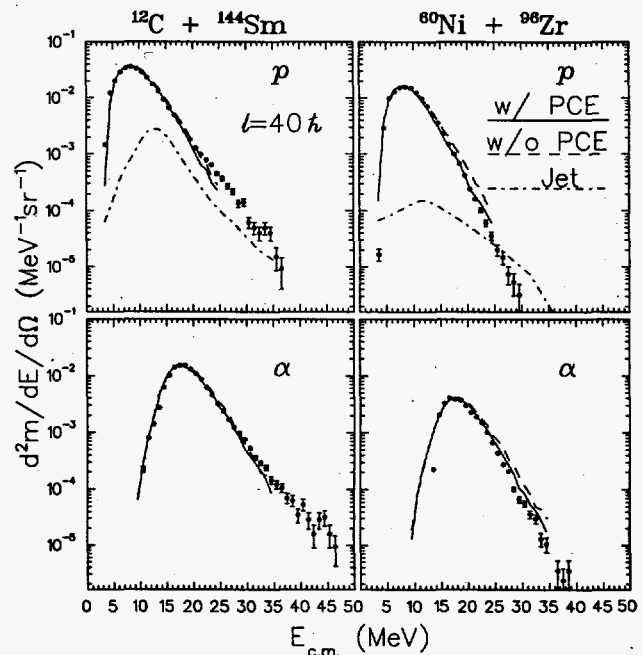


FIG. 2. Upper panels: Proton spectra for  $^{12}\text{C}+^{144}\text{Sm}$  and  $^{60}\text{Ni}+^{96}\text{Zr}$ . The dashed curve is for statistical model calculations without pre-compound evaporation (PCE). The solid curve is the result of calculations considering particle evaporation during formation. The contribution of pre-equilibrium jet particles is shown by the dash-dotted curves. Lower panels:  $\alpha$ -particle spectra for  $^{12}\text{C}+^{144}\text{Sm}$  and  $^{60}\text{Ni}+^{96}\text{Zr}$ .

Before pursuing the causes for the differences in the particle spectra, comparison between the data and statistical model calculations using the Monte Carlo code EVAP [8] assuming all particle evaporation follows compound nucleus formation is presented here first. In order

**DISCLAIMER**

**Portions of this document may be illegible  
in electronic image products. Images are  
produced from the best available original  
document.**

## DISCLAIMER

This report was prepared as an account of work sponsored by an agency of the United States Government. Neither the United States Government nor any agency thereof, nor any of their employees, makes any warranty, express or implied, or assumes any legal liability or responsibility for the accuracy, completeness, or usefulness of any information, apparatus, product, or process disclosed, or represents that its use would not infringe privately owned rights. Reference herein to any specific commercial product, process, or service by trade name, trademark, manufacturer, or otherwise does not necessarily constitute or imply its endorsement, recommendation, or favoring by the United States Government or any agency thereof. The views and opinions of authors expressed herein do not necessarily state or reflect those of the United States Government or any agency thereof.

to be assured that the spin window up to  $l_c^{ER}$  was being filled the ER cross section for  $^{60}\text{Ni}+^{96}\text{Zr}$  was extrapolated from Ref. [9]. The ER cross section for  $^{12}\text{C}+^{144}\text{Sm}$  was measured in a separate experiment which will be reported elsewhere. The  $l_c^{ER}$  extracted from the ER cross sections was  $l_c^{ER} = 57\hbar$  which agrees with an estimate by the rotating liquid drop model [10]. The calculated ER cross sections using the Sierk fission barrier [11] and  $a_f/a=1.07$  agree with the experimental measurements. A level density parameter of  $a=A/10$  was used to reproduce the high energy slope of the pre-equilibrium emission corrected data for the  $^{12}\text{C}+^{144}\text{Sm}$  reaction whereas  $a=A/8$  was needed for the  $^{60}\text{Ni}+^{96}\text{Zr}$  reaction. Some theoretical models show that for mass  $A \simeq 150$  at excitation energies near 100 MeV the level density parameter is  $a=A/10$  [12]. In order to reproduce the peak energy of the particle spectra, an emitter deformation was introduced to lower the Coulomb barrier for charged particle emission [13]. Transmission coefficients and the yrast line were calculated assuming a prolate shape emitter. Good agreement with the data was achieved by a deformation parameter  $\beta_2 = 0.25$ . This is shown by the solid curves in Fig. 1.

Since the corrections discussed above cannot account for the discrepancies between different entrance channels, the possibility of differences in the formation leading to the different spectra is examined. A one-body dissipation code HICOL [6] was used to estimate the amalgamation time of the compound formation. The amalgamation times for the  $^{60}\text{Ni}$ -induced reaction are two to four times longer than those of the  $^{12}\text{C}$ -induced reactions as shown in the top panel of Fig. 3. The excitation energy as a function of time is plotted at the mean spin,  $l \simeq 40\hbar$ , of the reaction in the bottom panel. Although somewhat faster for the lighter projectile system  $^{12}\text{C}+^{144}\text{Sm}$ , energy dissipation occurs rather rapidly compared to shape equilibrium. For the  $^{60}\text{Ni}+^{96}\text{Zr}$  system the shape equilibration time,  $\sim 50 \times 10^{-22}$  s, is significantly longer than  $20 \times 10^{-22}$  s calculated evaporative lifetime of the composite system. Therefore, particle evaporation during this period should be considered. It should be noted that these evaporated particles are to be distinguished from those emitted by the Fermi jet mechanism mentioned above as the pre-equilibrium emission. They will be called the pre-compound evaporation or evaporation during formation below. A simplified model which uses a statistical theory to account for particle evaporation during the formation period was devised. In the present model, the formation time was divided into several time intervals comparable to or less than the length of the lifetime as shown in Fig. 3. The lifetime of the composite system in a time interval was calculated using the average excitation energy and the average shape, given by HICOL, of that time interval. The probability of the dinuclear system without evaporating a particle follows the decay law,  $\exp(-\Delta t/\tau)$  where  $\Delta t$  is the duration of a time interval and  $\tau$  is the lifetime. If a particle was evap-

orated, the excitation energy of the dinuclear system will be reduced accordingly. Since  $\Delta t$  is very short, the possibility of emitting a second particle in the same time interval is negligible. Only one particle evaporation in each time interval was considered. This generated an input distribution, nuclei of different masses and excitation energies, for the next time interval. Following the same procedure, the calculations were performed throughout the the formation stage until the system reached amalgamation. It should be remembered that the statistical model parameters for a dinuclear system during formation are not known. Additionally, the system was not in equilibrium. The results from a statistical model can only be used as an estimate. In order to simplify the calculations, several approximations were made. Only secondary emission following neutron evaporation was considered in the calculations, since the dominant evaporation was neutrons and the average excitation energy carried away by a neutron was estimated to be only a few MeV less than that removed by protons and  $\alpha$ -particles. The level density parameter was chosen to be  $a=A/10$  and fixed throughout the calculations. These approximations were made in order to avoid introducing further free parameters.

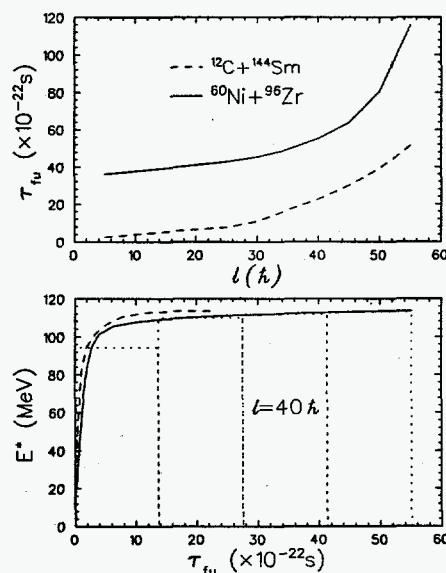


FIG. 3. Top panel: Amalgamation time as a function of angular momentum. Bottom panel: Excitation energy as a function of amalgamation time for  $l = 40\hbar$ . The solid curve is for  $^{60}\text{Ni}+^{96}\text{Zr}$  and the dashed curve is for  $^{12}\text{C}+^{144}\text{Sm}$ . The dotted lines show how the amalgamation period was divided to estimate pre-compound evaporation.

When the system has amalgamated, a distribution of equilibrated compound nuclei was produced rather than only  $^{156}\text{Er}$ . The decay of the equilibrium compound nuclei was calculated for the distribution of the corresponding excitation energy by the statistical model in a standard way. The light-charged particle spectra were

summed and weighted by the relative population of the compound distribution. Again, transmission coefficients were calculated for a prolate deformed emitter with a deformation parameter  $\beta_2=0.25$ . The results are shown in Fig. 2. The calculations taking into account the effect of formation time are shown by solid curves while without the effect of formation are shown by dashed curves. The contribution of the pre-equilibrium jet particles was included in those curves. For  $^{12}\text{C}+^{144}\text{Sm}$ , very little difference between the calculations can be seen. Either calculation is in good agreement with the data. For  $^{60}\text{Ni}+^{96}\text{Zr}$ , the data are well described by calculations including pre-compound evaporation. Without considering the effect of formation, the slope differs dramatically from the data. The cooling of the compound nucleus due to particle evaporation during a long formation time can be seen. The results are similar for the  $\alpha$ -particle spectra. At present, the Fermi jet model used is not able to predict pre-equilibrium emission for  $\alpha$ -particles. However, the inclusion of particle evaporation during formation in the calculations is qualitatively in better agreement with the data for both reactions. For the  $^{12}\text{C}$ -induced reactions, calculations with or without pre-compound evaporation gave similar results.

Some discrepancies between the calculations and data can still be seen in the  $\alpha$ -particle spectrum of the  $^{60}\text{Ni}$ -induced reaction. The amalgamation time for  $^{60}\text{Ni}+^{96}\text{Zr}$  as a function of angular momentum predicted by HICOL is linear for  $l \leq 30\hbar$ . It increases sharply with angular momentum for  $l > 30\hbar$ . The calculations were performed at the mean spin of the reaction,  $l = 40\hbar$ , only. More particle evaporation is expected at higher angular momentum which corresponds to longer amalgamation times. Moreover, the partial cross section  $\sigma_l$  at higher angular momentum contributes more to the total ER cross section because of the  $(2l + 1)$  factor. On the other hand, HICOL might underpredict the amalgamation time [1].

The level density parameter used in estimating the evaporation during formation was  $a=A/10$ . If a value of  $A/15$  was used as in Ref. [2], more particle evaporation during formation will take place. This will result in a lower equilibrium temperature for the compound nuclei. For the  $^{12}\text{C}$ -induced reaction, the level density parameter at equilibrium is  $a=A/10$ . The average excitation energy of any time interval in the formation calculation is at most 20 MeV less than the full excitation energy. The inverse level density parameter  $K=A/a$  should be slightly less than, if not equal to, 10 during amalgamation according to the temperature dependent level density study [12]. On the other hand, systematics of the ratio  $a_f/a \geq 1$  [14] implies that the level density parameter at large deformation is often greater than that of a sphere. The inverse level density parameter  $K$  should be less for a deformed nucleus. Nevertheless, the level density of a non-equilibrated dinuclear system is unknown. From the good agreement between the data and the model calcu-

lations obtained, the chosen value of  $a=A/10$  should be fairly reasonable.

The entrance channel effects, due to a long formation time, observed in this study are fairly moderate. The lifetime of a composite system is estimated to increase by an order of magnitude when the excitation energy decreases from 113 to 56 MeV. It is therefore somewhat surprising that similar effects were observed in some (but not all) experiments performed at excitation energies near 56 MeV.

In summary, different spectral shapes from the  $^{156}\text{Er}$  compound nucleus decay were observed for different entrance channels. The proposed explanation for the softness of the particle spectra for  $^{60}\text{Ni}+^{96}\text{Zr}$  is that due to a long amalgamation time particle evaporation during formation reduces the equilibrium excitation energy of the compound nucleus. Calculations taking into account the effect of the long formation time given by a one-body dissipation model are in good agreement with the experimental data.

We wish to thank the accelerator staff for providing the beams. We also thank the staff of the electronics shop and machine shop for technical assistance. This work was supported by the U. S. Department of Energy.

- 
- [1] M. Thoennessen, Nucl. Phys. A599, 1c(1996).
  - [2] M. Thoennessen, J. R. Beene, F. E. Bertrand, C. Baktash, M. L. Halbert, D. J. Horen, D. G. Sarantites, W. Spang, and D. W. Stracener, Phys. Rev. Lett. 70, 4055(1993).
  - [3] W. Kühn, P. Chowdhury, R. V. F. Janssens, T. L. Khoo, F. Haas, J. Kasagi, and R. M. Ronningen, Phys. Rev. Lett. 51, 1858(1983).
  - [4] B. Fornal *et al.*, Phys. Rev. C 42, 1472(1990).
  - [5] N. Bohr, Nature (London) 137, 344(1936).
  - [6] H. Feldmeier, Rep. Prog. Phys. 50, 915(1987).
  - [7] S. J. Luke, R. Vandenbosch, and J. Randrup, Phys. Rev. C 48, 857(1993).
  - [8] N. G. Nicolis, D. G. Sarantites, and J. R. Beene, computer code EVAP (unpublished).
  - [9] R. V. F. Janssens, R. Holzmann, W. Henning, T. L. Khoo, K. L. Lesko, G. S. F. Stephans, D. C. Radford, A. M. van den Berg, W. Kühn and, R. M. Ronningen, Phys. Lett. B 181, 16(1986).
  - [10] S. Cohen, F. Plasil, and W. J. Swiatecki, Ann. Phys. 82, 557(1974).
  - [11] A. J. Sierk, Phys. Rev. C 33, 2039(1986).
  - [12] S. Shlomo and J. B. Natowitz, Phys. Rev. C 44, 2878(1991).
  - [13] J. R. Huizenga, A. N. Behkami, I. M. Govil, W. U. Schröder, and J. Töke, Phys. Rev. C 40, 668(1989).
  - [14] W. Reisdorf, Z. Phys. A 300, 227(1981).